



# CHALMERS

## Chalmers Publication Library

### **Verification of the Rician K-factor-based uncertainty model for measurements in reverberation chambers**

This document has been downloaded from Chalmers Publication Library (CPL). It is the author's version of a work that was accepted for publication in:

**IET Science, Measurement & Technology (ISSN: 1751-8830)**

Citation for the published paper:

Chen, X. ; Kildal, P. ; Carlsson, J. (2015) "Verification of the Rician K-factor-based uncertainty model for measurements in reverberation chambers". IET Science, Measurement & Technology, vol. 9(5), pp. 534-539.

<http://dx.doi.org/10.1049/iet-smt.2014.0344>

Downloaded from: <http://publications.lib.chalmers.se/publication/222083>

Notice: Changes introduced as a result of publishing processes such as copy-editing and formatting may not be reflected in this document. For a definitive version of this work, please refer to the published source. Please note that access to the published version might require a subscription.

Chalmers Publication Library (CPL) offers the possibility of retrieving research publications produced at Chalmers University of Technology. It covers all types of publications: articles, dissertations, licentiate theses, masters theses, conference papers, reports etc. Since 2006 it is the official tool for Chalmers official publication statistics. To ensure that Chalmers research results are disseminated as widely as possible, an Open Access Policy has been adopted. The CPL service is administrated and maintained by Chalmers Library.

(article starts on next page)

# Verification of the Rician K-factor Based Uncertainty Model for Measurements in Reverberation Chambers

Xiaoming Chen, [xiaoming.chen@qamcom.se](mailto:xiaoming.chen@qamcom.se)

Qamcom Research & Technology, Gothenburg, Sweden

Per-Simon Kildal, [per-simon.kildal@chalmers.se](mailto:per-simon.kildal@chalmers.se)

Department of Signals and Systems, Chalmers University of Technology, Gothenburg, Sweden

Jan Carlsson, [jan.carlsson@sp.se](mailto:jan.carlsson@sp.se)

Electronics department, SP Technical Research Institute of Sweden, Borås, Sweden

***Abstract***—Measurements in reverberation chamber (RC) produce data that are random, and therefore they need to be processed from the statistical point-of-view for obtaining the desired characteristics and the accuracy. The complex channel transfer function in the RC follows complex Gaussian distribution provided that the RC is well stirred. We have recently presented a new uncertainty model based on the presence of an unstirred component of the transfer function, which was modelled by introducing an average Rician K-factor. The model was validated in two RCs with translating mode-stirring plates, being able to correctly describe the improvement in accuracy by rotating the antenna under test, and by blocking the line-of-sight between this and the fixed RC antenna(s). In the present paper we apply this uncertainty model to four RCs with different settings (e.g., RC volumes, number of plates or fixed RC antennas, translating and rotating mode-stirrers, etc.). For each RC, we examine the measurement uncertainty under different loading conditions. In order to repeat (during the different measurements) the actual mode-stirrer positions at which the transfer function is sampled, we conduct all the measurements with stepwise (instead of continuous) mode stirring. The model is shown to work well for all the cases.

## I. INTRODUCTION

Reverberation chambers (RCs) have been used for electromagnetic compatibility (EMC) [1] testing for more than two decades. Over the past decade, RCs have found new applications in characterizing multi-port antennas for multiple-input multiple-output (MIMO) systems [2] and over-the-air (OTA) testing of wireless devices [3]. Such measurements are incomplete without any

analysis of the measurement uncertainty. The RC measurements are random in nature, so both the desired randomness and the measurement errors must be analysed by using statistics. It is common practice to assume that the transfer function ( $S_{21}$  or the normalized  $S_{21}$  by calibrating out the antenna mismatches  $S_{11}$  and  $S_{22}$  for a two-port network) through a well-stirred chamber has a complex Gaussian distribution, and that the measurement error is related to the accuracy by which we can determine the average transfer function during a stirring cycle [4] for an arbitrary location and orientation of the antenna under test. Traditionally, this is determined from the effective number of independent samples of the transfer function, e.g., using the autocorrelation function (ACF) method [5], [6] (or its multivariate version [7]), based on autoregressive models [8] or the maximum entropy approach [9]. Nevertheless, these studies offer limited insight into how to improve the measurement uncertainty in the RC. Therefore, the paper [10] proposed to describe the transfer function in terms of two contributions: A desired stirred component and an undesired unstirred component. The stirred component has a complex Gaussian distribution and is strongly dominating in a well-stirred chamber, and the unstirred component becomes non-negligible in an RC with ineffective mode-stirring or heavy loading. The stirred and unstirred components result in a Rician distribution of the total complex transfer function. The Rician distribution is commonly characterized by a so-called K-factor, representing the ratio between the power of the unstirred component and the average power of the desired stirred component. The K-factor can normally not be removed by conventional mode stirring. Thereby, the K-factor represents a residual error that will be present even if the chamber is well stirred. Furthermore, in order to achieve a small measurement uncertainty it is not sufficient only with a large number of independent samples. The K-factor must in addition be small.

Based on this observation, the RC uncertainty in the overmoded regime (e.g., at high frequency where the mode density is large) can be improved by reducing either the effect of the K-factor or the K-factor itself. The effect of the K-factor is reduced by platform and polarisation stirring [2], by which the unstirred component takes on different values during the stirring cycle by mounting it on a rotatable platform (platform stirring) and switching between different RC-fixed antennas. The latter is called polarization stirring if the RC-fixed antennas have orthogonal polarizations. This is demonstrated very well in [10] and earlier papers. A major contributor to the K-factor itself is the direct coupling between the RC-fixed antenna and the antenna under test [11]. This is in OTA testing (where non-directive antennas are used) mainly due to a line-of-sight (LOS) component between the two antennas, and it can therefore easily be reduced by blocking the LOS path between the RC-fixed antenna and the antenna under test (AUT) with a metal shield. This was also demonstrated to work well in [10].

Platform and polarisation stirrings were used in the chambers evaluated in [10]. Therefore, the model made use of an average K-factor in the uncertainty model, i.e., the K-factor was averaged over the different platform positions and RC-fixed antennas.

OTA testing involves nowadays measuring the bit error rate (BER) [12], [13] and the throughput [14] of wireless devices or radar [15], and then the measurement uncertainty needs to be much better than for EMC tests. All these applications require calibration of the RC by performing a reference measurement to determine the average power transfer function  $P_{ref}$  (averaged over all the stirring samples). Thus, the measurement uncertainty of  $P_{ref}$  affects the overall measurement accuracies, and it is reasonable to assume that the overall standard deviation (STD) is  $\sqrt{2}$  times the STD of  $P_{ref}$  if the calibration and tests have been done under the same stirring conditions. [Denote the average power transfer function of the device under test (DUT) before calibration as  $P_{DUT}$ . It is easy to show by first-order Taylor expansion that the STD of  $P_{DUT}/P_{ref}$  approximately equals the sum of the STDs of  $P_{DUT}$  and  $P_{ref}$ . Provided that the DUT measurement has the same uncertainty as the reference measurement, it is obvious that the STD of  $P_{DUT}/P_{ref}$  is approximately  $\sqrt{2}$  times of the STD of  $P_{ref}$ .] The uncertainty of  $P_{ref}$  is given by the STD of several measurements of  $P_{ref}$  with the reference antenna in different locations and orientations. We will here use 9 different measurements, the same as in [10].

The uncertainty model proposed in [10] was till now only verified in two RCs with translating mode-stirring plates. In the present work we apply the uncertainty model (with necessary modifications) to four different RCs. These are the Bluetest HP, RTS60 and RTS90 chambers, and an RC at SP Technical Research Institute of Sweden, Borås, Sweden. The first two RCs were introduced in [10], while the RTS90 chamber is an enlarged version of the RTS60 chamber. The SP chamber is a larger RC, equipped with a rotating paddle (instead of translating plates) as the mode stirrer. All chambers make use of platform stirring.

## II. K-FACTOR BASED UNCERTAINTY MODEL

The STD of the average power transfer function  $P_{ref}$  in an RC is in [10] assumed to be given by the combined STDs of the two physical contributions to it, which was described in the introduction, i.e. the stirred or non-LOS (NLOS) contribution, and the unstirred or LOS contribution. The former contribution has a complex Gaussian probability distribution in a well-stirred chamber, and the average received power is given by Hill's formula [16], showing proportionality with the free space total radiation efficiency, independently of the orientation and location of the AUT. The estimation of this average has according to classical theory of Gaussian processes an STD of [4]

$$N_{LOS} = 1/\sqrt{M_{ind}}$$

where  $M_{ind}$  is the number of independent samples if the transfer function only had stirred components. The LOS contribution will depend on where in the chamber the antenna is located during the measurements, and its orientation. However, if the antenna under test has an arbitrary orientation inside the chamber, and if we neglect variations in the space attenuation, the expected power of this contribution will be the expected value of the radiation intensity function of the antenna over all directions. Thereby, this expected value will be independent of the shape of the radiation pattern and only depend on the total radiation efficiency, in the same way as

the NLOS contribution. However, the proportionality factors will be different. Therefore, we introduced in [10] a proportionality factor named the average Rician K-factor  $K_{av}$ .

When there is neither platform nor polarization stirring, and then the K-factor is determined by

$$K = \frac{|\overline{S_{21}}|^2}{|S_{21} - \overline{S_{21}}|^2}$$

where the overhead bar represents the average over all the stirrer positions (i.e., plate or paddle positions). Similarly, if we have polarization or platform stirring we can obtain the average K-factor  $K_{av}$  by averaging the Ks of all the platform and polarization stirring positions, as shown in (2) below.

Finally, if we assume that these two NLOS and LOS contributions to the stochastic transfer function are independent, the STD of the complete average power transfer function can be obtained from basic statistic theory as [10]

$$S = \sqrt{1/M_{ind} + K_{av}^2/M_{LOS}} / \sqrt{1 + K_{av}^2} \quad (1)$$

where  $M_{LOS}$  is the number of independent samples of the LOS contribution used to determine the average K-factor. This assumes that the antenna under test takes on a uniform distribution of angles of incidence and polarization during the platform and polarization stirring. This may not be the reality, but the formula should still be quite accurate for small antennas with low directivity.

This is easier to understand if we assume that the unstirred component actually is a direct LOS contribution. For each platform position and RC antenna, there will be a different K-factor which can be regarded as random. We do not know the exact K-factor, as this will depend on the orientation of the RC antenna and reference antenna relative to each other and the distance between them. However, when we perform a full rotation and switching over  $M_{LOS}$  positions and RC antennas, the average K-factor will of course converge towards a value given by the integral of the far field radiation intensity pattern of the reference antenna over the unit sphere (if the RC antennas are well separated). This value is in the perfect limit not dependent on pattern shape, and only on total radiation efficiency and average distance. Thus, the term  $K^2/M_{LOS}$  in (1) is more accurate when  $M_{LOS}$  is large. The average K-factor  $K_{av}$  in (1) is obtained by averaging the directly coupled power and the stirred power separately, and then taking the ratio between them. The averaging is in both cases taken over both the platform positions  $M_{pf}$  and fixed RC antennas  $M_{ant}$ . The overall formula is

$$K_{av} = \frac{\sum_{M_{pf}M_{ant}} |\overline{S_{21}}|^2}{\sum_{M_{pf}M_{ant}} |S_{21} - \overline{S_{21}}|^2} \quad (2)$$

where  $M_{LOS}$  can be expressed as

$$M_{LOS} = M_{pf}M_{ant,ind} \quad (3)$$

with  $M_{ant,ind} = M_{ant}$  for fixed RC antennas that are separated by at least half-wavelength and  $M_{ant,ind} = 2$  for two co-located fixed RC antennas of orthogonal polarization [10].

Another uncertainty model based on a similar idea is presented in [17], where it assumes a third uncertainty contribution, i.e., noise uncertainty and that NLOS, LOS and noise components follow Gaussian distributions with different variances. In this work, we assume the noise uncertainty contribution is negligible, compared to the other two contributions, and we focus only on the NLOS and LOS contributions.

Since the three stirring mechanisms (i.e., fixed RC antennas, platform, and plate/paddle) are independent, the total number of independent samples  $M_{ind}$  becomes

$$M_{ind} = M_{ant,ind} M_{stir,ind} M_{pf,ind} \quad (4)$$

where  $M_{ant,ind}$ ,  $M_{stir,ind}$ , and  $M_{pf,ind}$  are the independent numbers of samples from the fixed RC antennas, the mode stirrers, and the platform, respectively. Usually, the fixed RC antennas (if more than one) are made uncorrelated by putting them orthogonal to each other and with sufficient separation. In our case  $M_{ant,ind}$  equals the number of fixed RC antennas. Some models for  $M_{stir,ind}$  and  $M_{pf,ind}$  (for translating plates) are given in [10]. Note that (4) holds because the fixed RC antennas, platform, and plate/paddle stirring sequences are from three independent stirring mechanisms. It does not hold if the stirring sequences are from the same stirring mechanism, e.g., the independent sample number of two mode-stirrers is, in general, smaller than the product of the independent sample numbers of the two mode-stirrers [7], [18].

Traditional reverberation chambers have a rotating paddle instead of translating plates. The number of independent paddle positions is according to [5] given by

$$M_{stir,ind} = \min \left\{ M_{pad}, \frac{2R_{pad} \sin(2\pi / M_{pad}) M_{pad}}{\lambda / 2} \right\} \quad (5)$$

where  $M_{pad}$  is the number of paddle positions, and  $R_{pad}$  is the largest radius of the paddle. Arnaut [19] proposes a more heuristic approach for calculating  $M_{stir,ind}$ , by stating that the number of independent paddle positions equals the volume that the rectangular-shaped paddle sweep during the stirring cycle divided by the volume of a coherence cell (that is a cube with half-wavelength dimensions). This approach is very convenient to use for paddle with regular shape, i.e., a plate. However, for irregular paddles, the swept volumes are difficult to calculate; furthermore, [19] confines to analytical study of plate paddle only. It should be noted that any complex shape can be decomposed into regular building surfaces. Hence it is possible to calculate the actual volume that the paddle sweeps. However, this involves detailed modeling of the paddle and nontrivial transformation from its irregular shape to building surfaces. Since the ultimate goal of this uncertainty work is to present an uncertainty model that is simple

to use (and should not depend on the actual shape of the mode-stirrer), for simplicity, we use (5) in this paper to model the number of independent samples for the RC with the rotating stirrer.

### III. DESCRIPTION OF MEASUREMENTS

In order to validate the K-factor based uncertainty model (1), we performed extensive measurement campaigns in four RCs with different sizes and stirring mechanisms. The four RCs are Bluetest HP, RTS 60, RTS 90, and SP RC as explained at the end of the introduction (see also Fig. 1 and Table I).

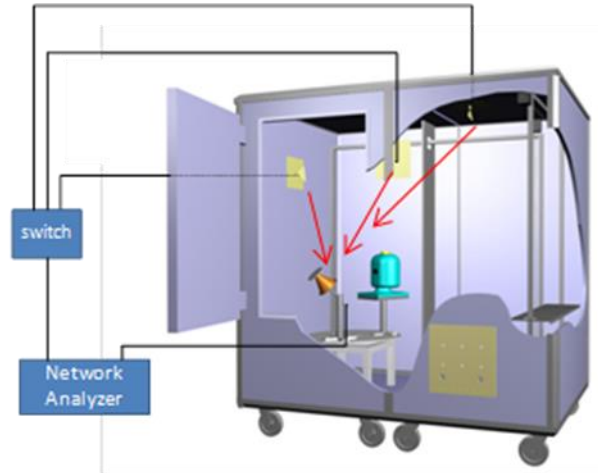


Fig. 1 Drawing of Bluetest HP RC, and photo of the turn-table platform and the paddle of the SP RC.

The Bluetest RTS60 RC has the same size as the HP RC, and they are also otherwise the same, except that the RC-fixed antennas of the RTS60 RC are hidden behind a metal shield located to the right side of the turntable in the chamber, and that the vertical plate

stirrer of the HP RC is changed into a horizontal plate stirrer that moves along the ceiling of the RTS60. The Bluest RTS90 RC is basically an enlarged version of the RTS60 RC. For the sake of conciseness, RTS60 and RTS90 RCs are not shown here.

Measurements in the Bluetest HP RC were performed from 500 to 3000 MHz. The RC has two mode-stirring plates, a turntable platform, and three RC-fixed antennas mounted on three orthogonal walls. On the platform, a wideband discone reference antenna is mounted, which will rotate along with the platform during the measurements. This is the already described platform stirring, and it is applied in all of the four RCs. The RC-fixed wall antennas are wideband half-bow-tie monopole-like antennas. During the measurement, the turntable platform was moved stepwise to 20 platform stirring positions evenly distributed over one complete platform rotation; at each platform-stirring position the two plates were simultaneously moved in a stepwise manner to 50 positions (equally distributed over the total distances that they can travel along two RC walls). At each stirrer position and for each wall antenna a full frequency sweep was performed by a vector network analyzer (VNA) with a frequency step of 1 MHz, during which the scattering parameter (S-parameter) was sampled as a function of frequency and stirring position. Hence, for this measurement setup, we have 3 wall antennas, 50 plate-stirring positions, and 20 platform-stirring positions, i.e.  $M_{ant} = 3$ ,  $M_{st} = 50$ , and  $M_{pf} = 20$ .

The configurations of RTS 60 and RTS 90 are similar to that of the HP RC, except that the RC-fixed antennas are placed behind a metallic shield in order to reduce the direct coupling also called LOS contribution (and therefore they are not wall-mounted as in RTS 60 and RTS 90). The measurement setups are rather similar to that of the HP RC. The measurements in the Bluetest RTS 60 RC were also performed from 500 to 3000 MHz yet with a frequency step of 2 MHz. To reduce the measurement time, the number of plate-stirring positions were reduced to 25, i.e.,  $M_{ant} = 3$ ,  $M_{st} = 25$ , and  $M_{pf} = 20$ .

Table I: The four reverberation chambers used for validating the uncertainty Model

	Size	Configuration
Bluetest HP RC	1.8 m × 1.7 m × 1.2 m	3 wall antennas, 1 turntable platform, 2 translating plates
Bluetest RTS60	1.8 m × 1.7 m × 1.2 m	3 fixed RC antennas, 1 turntable platform, 2 translating plates
Bluetest RTS90	3.3 m × 4.2 m × 2.5 m	4 fixed RC antennas, 1 turntable platform, 6 translating plates
SP RC	3.0 m × 2.5 m × 2.5 m	3 wall antennas, 1 turntable platform, 1 rotating paddle

Since RTS 90 is an enlarged version of RTS 60. We are for this case more interested in its performance at the low frequency. Thus the measurements in RTS 90 were performed from 250 to 1500 MHz with a frequency step of 2 MHz. To fully examine the minimum possible uncertainty in RTS 90, we oversample the RC by using  $M_{ant} = 4$ ,  $M_{st} = 50$ , and  $M_{pf} = 40$ .

The SP RC has a rotating paddle (instead of translating plates in the Bluetest RCs), a turntable platform (see Fig. 1), and three wall-mounted RC-fixed antennas. The measurements were performed from 500 MHz to 2000 MHz with a frequency step of 1 MHz. For this measurement setup, we have 3 wall antennas, 50 plate-stirring positions, and 20 platform-stirring positions, i.e.  $M_{ant} = 3$ ,  $M_{st} = 30$ , and  $M_{pf} = 10$ .

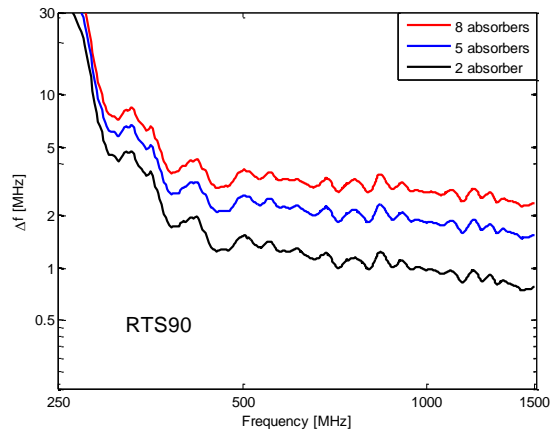
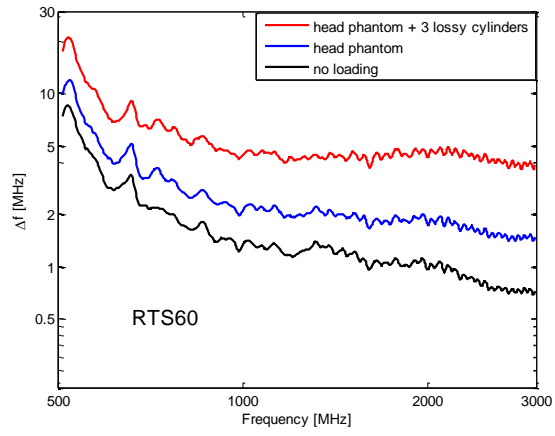
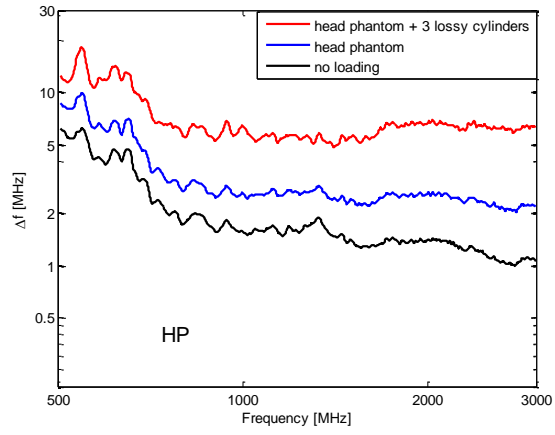
Before showing the uncertainty results, we would like to present an important parameter of the RC, i.e., the average mode bandwidth. This can be determined from the level of the transfer function by using Hill's formula (eq. (6) in [10]), giving

$$\Delta f = c_0^3 e_{rad1} e_{rad2} / (16\pi^2 f^2 V \overline{|S_{21}|^2}) \quad (6)$$

where  $e_{rad1}$  and  $e_{rad2}$  are the total radiation efficiencies of the transmitting and receiving antennas, respectively,  $S_{21}$  is the sampled transfer function between the transmitting RC-fixed antenna and receiving antennas under test, the overhead bar represents the average over all the stirring positions (i.e., RC-fixed antennas, platform positions, and stirrer positions),  $V$  is the RC volume, and  $c_0$  is speed of light. Note that the original formula in the work of Hill et al. [16] expresses the transfer function in terms of the quality-factor  $Q$  of the chamber rather than the average mode bandwidth, where  $\Delta f = f / Q$  with  $f$  being the frequency.

It should be noted that the average mode bandwidth equals the coherence bandwidth of the radio channel in the RC, as shown in [20]. By loading the RC, the average power transfer function  $\overline{|S_{21}|^2}$  decreases, and then (6) shows that the average mode bandwidth increases inversely proportional to  $\overline{|S_{21}|^2}$ .

Fig. 2 shows the average mode bandwidths of the four different RCs and three different loadings, calculated from  $\overline{|S_{21}|^2}$  by using (6). Note that in Bluetest RCs, we have internal cables (connecting the mechanical switch and the RC-fixed antennas) that are not calibrated out in the VNA calibration. In the normal OTA test, the cable effect will be calibrated out by performing a reference measurement, which calibrated out the chamber together with the internal cable. However, the internal cables have to be calibrated out by performing separate measurements of the cables' insertion loss in order to correctly calculate the average mode bandwidth (6). As expected, the average mode bandwidth (coherence bandwidth) increases with increasing loading. The loadings for different RCs are summarized in Table II.



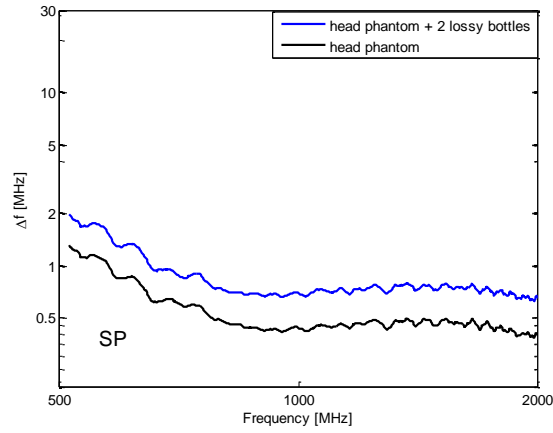
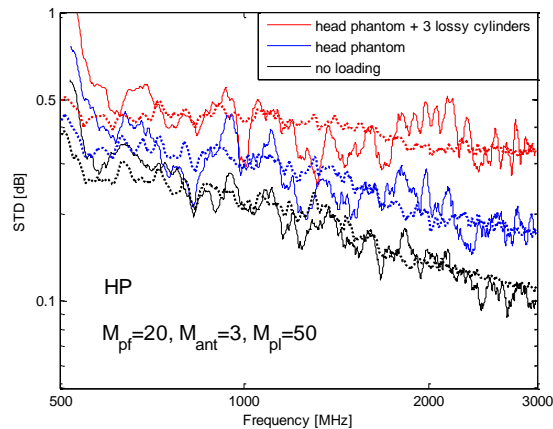


Fig. 2. Average mode bandwidths of the four different RCs.

Table II: The loadings used in the measurements of the four reverberation chambers. Note that since the main focus of this work is to validate the uncertainty model, the exact loss for each loading is not of interest. The loads are located in such a way that they do not block the LOS.

	Loadings
Bluetest HP RC	3 loading conditions: (1) no loading (2) head phantom (3) head phantom plus 3 lossy cylinders
Bluetest RTS60	3 loading conditions: (1) no loading (2) head phantom (3) head phantom plus 3 lossy cylinders
Bluetest RTS90	3 loading conditions: (1) 2 absorbers (2) 5 absorbers (3) 8 absorbers
SP RC	2 loading conditions: (1) head phantom (2) head phantom plus 2 lossy bottles



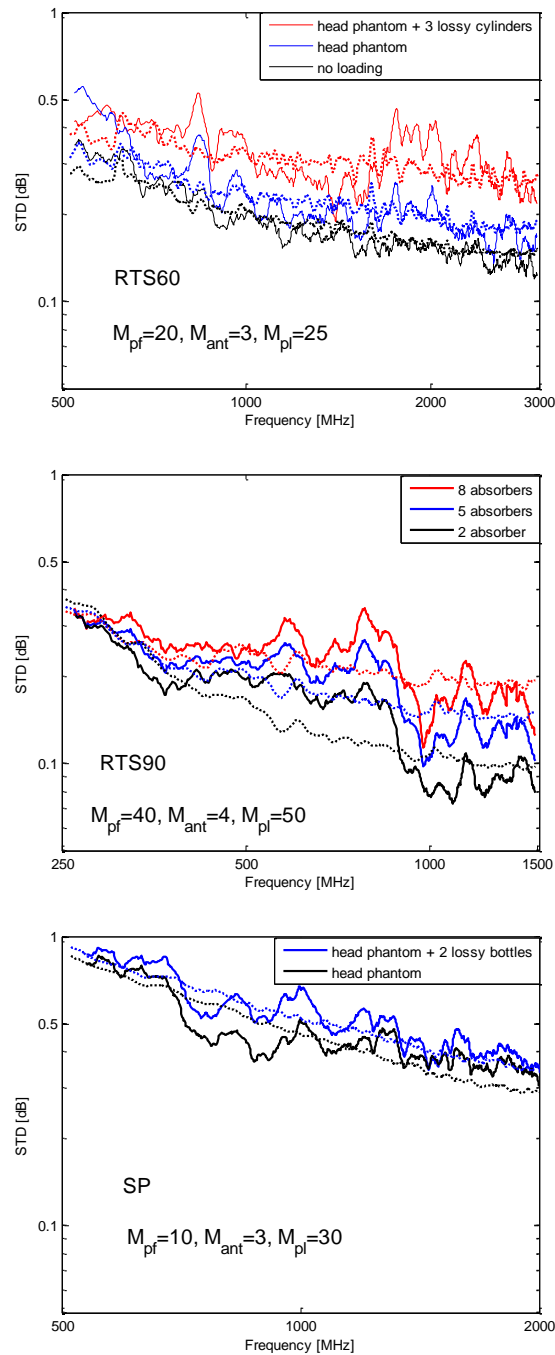


Fig. 3. Modelled and measured STDs of four different RCs. The solid curves represent measurements and the dotted curves correspond to the model. The numbers of turntable platform positions  $M_{pf}$ , RC-fixed antennas  $M_{ant}$ , and plate or paddle positions  $M_{pl}$  used are marked in their corresponding graphs.

In order to estimate the measurement uncertainty (in terms of STD of the average power transfer function  $P_{ref}$ ), the same measurement sequence was repeated nine times, each time with a different height/orientation of the discone antenna on the platform, i.e., the discone antenna on the platform was placed with three different heights and at each height it is placed with three different

orientations. This nine-measurement procedure was proposed in [10] for uncertainty assessment. The uncertainty of determining the STD is  $1/3$ . We smoothen this uncertainty of the estimate of the STD by averaging the square of the STD over a frequency bandwidth of 50 MHz, in the same way as in [10]. For clarity the calculated STD  $\sigma$  is plotted in dB using the following dB-transformation, which is symmetric in  $+\sigma$ ,

$$S_{dB} = 5 \log((1 + S) / (1 - S)). \quad (7)$$

The plotted values in the graphs in are the estimated STDs of  $P_{ref}$ , not the overall uncertainty in predicting quantities proportional to the radiation efficiency of the AUT. If we predict the  $P_{ref}$  by only one measurement, the accuracy of the radiation efficiency of the AUT based on one measurements of the AUT will be  $\sqrt{2}$  times larger. However, if we use  $P_{ref}$  based on averaging nine independent reference measurements, the measurement accuracy of the AUT will be only a factor  $\sqrt{1 + (1/9)} = 1.05$  times larger, so the presented STD is very representative of the actual chamber accuracies provided nine independent calibrations are averaged.

#### IV. RESULTS

In order to apply the uncertainty model (1), we need to estimate the average K-factor  $K_{av}$  and the independent number of RC-fixed antennas, platform positions, and stirrer positions. As mentioned in Sec. II, the fixed RC antennas for all the four RCs are uncorrelated, and therefore the independent number of RC-fixed antennas is simply the number of them. (Note that if the fixed RC antennas are correlated, one can resort to the diversity measure [21] for calculating the independent number of fixed RC antennas. The diversity measure for calculating the number of independent ports of a multi-port antenna under test has been applied to RC measurement in [22].) All the four RCs apply platform stirring, whose independent position can be estimated by (12b) in [10]. It was originally assumed that the independent plate positions should be bounded by the number of modes excited in the Bluetest HP and RTS60. However, it was found out by experiments that, without this bounding, better agreement was observed. Hence, for all the three Bluetest RCs (i.e., HP, RTS60 and RTS90), the number of independent plate positions equals the number of plate positions; and this is further verified by the good agreement of the RTS90 chamber (see Fig. 3). This means that the maximum number of independent stirrer positions at all frequencies is so large that this corresponding minimum NLOS uncertainty always is much smaller than uncertainty due to the NLOS-contribution.

For the SP RC however, the paddle only occupies a small portion of the RC volume (i.e., the paddle is less effective in interacting with the Electromagnetic field in the RC), so the effectiveness of the paddle is not as good as the Bluetest RCs. Therefore, we bounded the independent paddle positions by using (5) when we evaluated the STD using the theoretical formula (1).

In order to know at which positions the S-parameters are sampled, we conducted all the measurements with stepwise mode-stirring (i.e., the plates or paddle move stepwise through a sequence of predefined positions or angles, at each position or

angle the mode-stirrer stop and the S-parameters are recorded accordingly). The stepwise measurements allow convenient processing of the measured data [10].

Fig. 3 shows the estimated standard deviations (STDs) of the average power transfer functions from the already-described nine-case-measurement uncertainty assessment procedure, together with the modelled STDs for the four RCs, respectively. The solid curves represent measurements and the dotted curves correspond to the model. It can be seen that, for all the four RC measurements, the measurement uncertainty degrades with increasing loading and improves with increasing frequency. Yet at high frequencies, there is a irreducible STD floor due to the presence of the K-factor. This phenomenon is more noticeable in the heavy loading case. In OTA applications, sometimes, the RC needs to be tuned to achieve a specific channel delay spread by loading the RC with lossy objects, see e.g., [13], [20]. The results of this work implies that extra care should be exerted in OTA tests to make sure that the loading does not degrade the measurement accuracy too much or to bear in mind what is the uncertainty level of the OTA testing for a specific loading. Note that the measurement campaigns were performed with some time span with the main intention to validate the uncertainty model in the different RCs. Hence, different loading conditions, sample numbers, and frequency ranges were used. However, it is safe to conclude that the RTS90 has the best measurement accuracy, even though it is operating in a lower frequency range. Anyway, we see from Fig. 3 that the model agrees with the measured uncertainties for all chambers. This validates the uncertainty model, and shows also that (5) as presented in [5] is a good predictor of the number of independent samples for rotating paddle-type stirrers.

## V. CONCLUSION

We have presented a K-factor based RC uncertainty model, which indicates that the average Rician K-factor represents a residual error for RC measurements. The model has been partially validated in two RCs with translating mode-stirrers only [10]. In this work, we further verified the uncertainty model by extensive measurement campaigns in four different RCs, including both translating and rotating mode-stirrers. The results show that the uncertainty model can well predict the measurement uncertainty not only for RCs with translating mode-stirrers but also for RCs with rotating mode-stirrers, in the latter case together with the number of independent stirrer positions described by (5) from [5]. The extension of the uncertainty model to RCs with rotating mode-stirrers is important in that many RCs are equipped with rotating mode-stirrers. Based on the good agreements between all the measurements and the uncertainty model, it is safe to conclude that the model is generally valid for arbitrary RC configurations.

## REFERENCES

- [1] Bäckström, M. L., Kildal, P.-S.: ‘Reverberation chambers for EMC susceptibility and emission analyses’, *Review of Radio Science* 1999-2002, 2002, pp. 429-452

- [2] Kildal, P.-S., Rosengren, K.: 'Correlation and capacity of MIMO systems and mutual coupling, radiation efficiency and diversity gain of their antennas: Simulations and measurements in reverberation chamber', *IEEE Communications Magazine*, 2004, 42, (12), pp. 102-112
- [3] Kildal, P.-S., Orlenius, C., Carlsson, J.: 'OTA Testing in Multipath of Antennas and Wireless Devices with MIMO and OFDM', *Proceedings of the IEEE*, 2012, 100, (7), pp. 2145-2157
- [4] Kostas, J. G., Boverie, B.: 'Statistical model for a mode-stirred chamber', *IEEE Trans. Electromagn. Compat.*, 1991, 33, (4), pp. 366-370
- [5] Wellander, N., Lunden, O., Bäckström, M.: 'Experimental investigation and mathematical modeling of design parameters for efficient stirrers in mode-stirred reverberation chambers', *IEEE Trans. Electromagn. Compat.*, 2007, 49, (1), pp. 94-103
- [6] Clegg, J., Marvin, A. C., Dawson, J. F., et al.: 'Optimization of stirrer designs in a reverberation chamber', *IEEE Trans. Electromagn. Compat.*, 2005, 47, (4), pp. 824-832
- [7] Gradoni, G., Mariani Primiani, V., Moglie, F.: 'Reverberation chamber as a multivariate process: FDTD evaluation of correlation matrix and independent positions', *Progress in Electromagnetics Research*, 2013, 133, pp. 217-234
- [8] Lemoine, C., Besnier, P., and Drissi, M.: 'Estimating the effective sample size to select independent measurements in a reverberation chamber', *IEEE Trans. Electromagn. Compat.*, 2008, 50, (2), pp. 227-236
- [9] Pirkel, R. J., Remley, K. A., Patané, C. S. L.: 'Reverberation chamber measurement correlation', *IEEE Trans. Electromagn. Compat.*, 2012, 54, (3), pp. 533-544
- [10] Kildal, P.-S., Chen, X., Orlenius, C., et al.: 'Characterization of Reverberation Chambers for OTA Measurements of Wireless Devices: Physical Formulations of Channel Matrix and New Uncertainty Formula', *IEEE Trans. Antennas Propag.*, 2012, 60, (8), pp. 3875 – 3891
- [11] Chen, X., Kildal, P.-S., Lai, S.-H.: 'Estimation of average Rician K-factor and average mode bandwidth in loaded reverberation chamber', *IEEE Antennas and Wireless Propagation Letters*, 2011, 10, pp. 1437-1440
- [12] Ferrara, G., Migliaccio, M., Sorrentino, A.: 'Characterization of GSM non-line-of-sight propagation channels generated in a reverberating chamber by using bit error rates', *IEEE Trans. Electromagn. Compat.*, 2007, 49, (3), pp. 467-473
- [13] Genender, E., Holloway, C. L., Remley, K. A., et al.: 'Simulating the multipath channel with a reverberation chamber: application to bit error rate measurements', *IEEE Trans. Electromagn. Compat.*, 2010, 52, (4), pp. 766-777
- [14] Chen, X., Kildal, P.-S., Gustafsson, M.: 'Characterization of Implemented Algorithm for MIMO Spatial Multiplexing in Reverberation Chamber', *IEEE Trans. Antennas Propag.*, 2013, 61, (8), pp. 4400-4404
- [15] Im, Y.-T., Ali, M., Park, S.-O.: 'Slow modulation behavior of the FMCW radar for wireless channel sounding technology',

- IEEE Trans. Electromagn. Compat., 2014, 56, (5), pp. 1229-1237
- [16] Hill, D. A., Ma, M. T., Ondrejka, A. R., et al.: 'Aperture excitation of electrically large, lossy cavities', IEEE Trans. Electromagn. Compat., 1994, 36, (3), pp. 169-178.
- [17] Remley, K. A., Pirkl, R. J., Shah, H. A., et al.: 'Uncertainty from choice of mode-stirring technique in reverberation-chamber measurements', IEEE Trans. Electromagn. Compat., 2013, 55, (6), pp. 1022-1030
- [18] Gradoni, G., Mariani Primiani, V., Moglie, F.: 'Reverberation chamber as a statistical relaxation process: entropy analysis and fast time domain simulations', International Symposium on Electromagnetic Compatibility, Rome, Italy, Sep. 2012, pp. 1-6
- [19] Arnaut, L. R.: 'Effect of size, orientation, and eccentricity of mode stirrers on their performance in reverberation chambers', IEEE Trans. Electromagn. Compat., 2006, 48, (3), pp. 600-602
- [20] Chen, X., Kildal, P.-S., Orlenius, C., et al.: 'Channel sounding of loaded reverberation chamber for Over-the-Air testing of wireless devices - coherence bandwidth and delay spread versus average mode bandwidth', IEEE Antennas Wireless Propag. Letters, 2009, 8, pp. 678-681
- [21] Ivrlac, M. T., Nossek, J. A.: 'Diversity and correlation in Rayleigh fading MIMO channels', in Proc. IEEE VTC2005-Spring, Stockholm, Sweden, May 2005, pp. 151-155
- [22] Chen, X., Kildal, P.-S., Carlsson, J.: 'Capacity characterization of Eleven antenna in different configurations for MIMO applications using reverberation chamber', 6th European Conference on Antennas and Propagation, Prague, Czech, Mar. 2012, pp. 1571-1575